RSC Advances

PAPER

View Article Online
View Journal | View Issue

Cite this: *RSC Adv.*, 2021, **11**, 7913

Synthesis of a new Ag^+-decorated Prussian blue analog with high peroxidase-like activity and its application in measuring the content of the antioxidant substances in *Lycium ruthenicum* Murr.†

Linqi Cheng, ‡[a] Haoxue Ding, ‡[a] Chunying Wu,[a] Shuyu Wang[a] and Xueyan Zhan*[ab]

A new Prussian blue analog (PBA) that contains three metal elements and has peroxidase-like activity was synthesized by a simple method. Then, $AgNO_3$ solution was added slowly to the PBA solution under continuous stirring. We found that this synthesis method could be used to prepare other PBAs, and that the anchoring of Ag^+ on the surface of PBA could enhance the peroxidase-like activity of the material, suggesting potential applications for the Ag^+-decorated Prussian blue analog (Ag-PBA) in traditional Chinese medicine. Ag-PBA is a new type of multi-metal cubic nano-enzyme that exhibits good stability and excellent peroxidase-like activity; as such, it could catalyze the oxidation of 3,3′,5,5′-tetramethylbenzidine (TMB) in the presence of H_2O_2 and Ag-PBA. We then developed a new method to measure the content of antioxidant substances in Chinese herbs by using the excellent peroxidase-like activity of Ag-PBA. Using the Chinese herb *Lycium ruthenicum* Murr. as a model compound, we measured the content of the antioxidant substances in *Lycium ruthenicum* Murr. by this new method. After optimization of reaction temperature, concentrations of TMB and H_2O_2, and reaction time, the content of the antioxidant substances was measured and calculated in comparison with anthocyanidin standards. The results of the Ag-PBA method and the classical DPPH method were compared by a paired *t*-test, with no statistically significant difference found between the methods. Hence, these two methods can be used interchangeably, although the Ag-PBA method had the advantages of simplicity, rapidness, and good stability. Moreover, the Ag-PBA method has a low limit of quantification and a shorter reaction time, which are improvements on the DPPH method, and it is not necessary to avoid light. Therefore, we anticipate that the Ag-PBA method may be used widely for the measurement of the content of antioxidant substances in Chinese herbs.

Received 10th December 2020
Accepted 4th February 2021

DOI: 10.1039/d0ra10396a

rsc.li/rsc-advances

1. Introduction

Enzymes are a class of biocatalysts that play essential roles in metabolism, nutrition, and energy conversion in organisms. They are also used in many applications, including in bioengineering, agriculture, the food industry, and environmental protection.[1] However, the inherent disadvantages to the use of natural enzymes, such as complicated extraction and purification steps, high costs, poor stability, and difficulties in recovery and storage, have limited their use.[2] To solve these problems, researchers have focused on artificial enzyme mimetics, especially nano-mimetic enzymes, which generally have the advantages of easily controllable preparation, low cost, high stability, flexible structure design, and easy preparation.[3–5] Moreover, the catalytic activity of nano-mimetic enzymes can be adjusted by various approaches, including surface modification and alteration of particle size. These qualities have encouraged scientists to explore various nanomaterials that can imitate the catalytic properties and mechanism of natural enzymes.[5] However, the catalytic activity of nano-mimetic enzymes is generally low. Therefore, the identification of methods to improve the catalytic activity of nano-mimetic enzymes is a major problem for researchers studying these enzymes.[6]

[a]*Beijing University of Chinese Medicine, Beijing 102400, China. E-mail: snowzhan@bucm.edu.cn*

[b]*Beijing Key Laboratory for Process Control and Quality Evaluation of Traditional Chinese Medicine, Beijing 102400, China*

† Electronic supplementary information (ESI) available. See DOI: 10.1039/d0ra10396a

‡ These authors contributed equally to this work.

Prussian blue (PB), also known as ferric ferrocyanide ($Fe_4^{III}[Fe^{II}(CN)_6]_3$), is a material that has been used for coordination for many years; the first studies on this material date from the early 18th century.[7] The crystalline structure of PB was determined to be a basic cubic structure consisting of alternating iron(II) ions and iron(III) ions located on a face-centered cubic lattice. The carbon atoms surround the iron(II) ions, and the iron(III) ions are surrounded octahedrally by nitrogen atoms.[7–9] Recently, PB has been widely investigated for batteries, sensors, and catalysis owing to its excellent electrochemical and optical properties.[10–13] Furthermore, because of its distinct advantages of good biocompatibility, hollow mesoporous structure, and other unique properties, PB nanoparticles have also been used widely in biomedicine and biosensors.[14–17] Moreover, PB crystals consist of Fe^{2+} and Fe^{3+} coordinated by CN^- bridges, which have peroxidase-like activity. Owing to its limited dispersibility and inherent color that interferes with measurement, it is not easy to directly apply PB with peroxidase-like activity in colorimetric biosensing. However, it can be introduced into metal–organic frameworks (MOFs) to develop a stable enzyme-mimetic system; such compounds have many potential applications.[18] Consequently, the synthesis of PB analogs (PBAs) with MOF structures and high peroxidase-like activity has been investigated extensively.[17,19,20] For example, Vazquez-Gonzalez *et al.* synthesized several PBAs and compared their peroxidase-like activity.[20]

Based on the synthetic strategies, Li *et al.* categorized MOF-based nanozymes into four classes.[18] PBA is in the "MOF-based composites" category,[18] which exhibits the inherent properties of MOFs. MOFs are porous crystalline materials, in which metal ions/clusters are coordinated with organic linkers; their inherent advantages for catalysis include an abundance of metal active sites, high porosity, diverse structures, and tunable chemical composition.[18,21] Moreover, MOFs have ample accessible catalytic sites and inherent enzyme-mimetic properties, which arise from the regular arrangement of organic ligands and metal nodes in their structures. Therefore, MOFs have developed rapidly over the last few decades. For example, Chen *et al.* synthesized a type of MOF-derived Co_3O_4@Co–Fe oxide double-shelled nanocages with high peroxidase-like activity for chemo/biosensing and dye degradation.[22] Cheng *et al.* synthesized a series of MOF nanosheets and established a highly sensitive and selective diagnostic platform for the *in vivo* monitoring of heparin activity.[23]

Similarly, various methods have been used to synthesize PB nanoparticles and their analogs, such as straightforward solution methods, microemulsions, sonochemical methods, microwave-assisted methods, electrodeposition, selective chemical etching, and hydrothermal methods.[7,24–27] Among them, the straightforward solution method is a rapid process comprising simple mixing of the ligands and metal sources in a controlling agent (trisodium citrate dihydrate, TSCD) at room temperature. However, TSCD plays a vital role in the final formation and morphology of particles, worthy of further discussion.[24,28,29] Hu *et al.* proposed a simple method to control the size and morphology of PB nanoparticles by regulating the pH of the solution and the concentrations of $K_3[Fe(CN)_6]$ and polyvinylpyrrolidone (PVP).[27] Other methods require either acidic conditions and high temperatures or other equipment, such as microwave or electrochemical instruments.

Through the study of nano-mimetic enzymes, it has emerged that hybrid composite materials may be good catalysts as the combination of the respective properties of each component can lead to cooperatively enhanced functions.[30] We aimed to synthesize trimetallic PBA, which was proposed to combine the properties of the three individual metals to achieve high peroxidase-like activity. The synthesis of trimetallic PBA is likely to support the development of new and efficient catalysts. Moreover, there are few reports of the synthetic methods for PBAs with three metals. Thus, we aimed to propose a feasible method for the synthesis of trimetallic PBA with high peroxidase-like activity and to provide a platform for the synthesis of other different trimetallic PBAs with high catalytic activity in future studies.

In this paper, we have proposed a simple method, which did not require heating or pH control of the solution, to synthesize a new PBA, a type of MOF-based composite, which contained three metals and showed good peroxidase-like activity. The synthesis method was convenient, economical, and environmentally friendly. Functional metal nanoparticles can be attached within MOFs cages/channels owing to the high porosity and flexibility of MOFs.[31] Ag nanoparticles, as functional metal nanoparticles, can be combined with other materials to form nanocomposites with good catalase-like activity.[32–35] Thus, we found that when Ag^+ was deposited on PBA, the peroxidase-like activity of PBA could be improved further. The anchorage of Ag^+ on the surface of nanozymes was utilized to enhance their standard activity. The deposition of Ag nanoparticles on PBA provides a naked catalytic surface with high catalytic activity, which could catalyze the oxidation of 3,3′,5,5′-tetramethylbenzidine (TMB) to ox-TMB in the presence of H_2O_2, along with a color change.[36] Ag^+-decorated PBA (Ag-PBA) exhibited excellent thermostability, storability, reusability, and good acid resistance in solutions with pH from 4.0 to 7.0. We anticipate that the described synthetic method can be used to prepare other trimetallic PBAs, and that these nano-enzymes may have practical applications in some fields, such as measuring the antioxidative activity of traditional Chinese medicines (TCMs).

To prove the feasibility of the use of Ag-PBA in TCM, we developed a new method to measure the content of the antioxidant substances in TCM herbs by using the excellent peroxidase-like activity of Ag-PBA. Using *Lycium ruthenicum* Murr. as an example, we measured the content of the antioxidant substances in *L. ruthenicum* Murr. by this new method. *L. ruthenicum* Murr., which belongs to the genus *Lycium* of the nightshade family, contains an abundance of anthocyanidins and is a perennial wild shrub in the arid areas of salinized deserts in the Qinghai-Tibet Plateau, China.[37] Anthocyanidins are a class of water-soluble

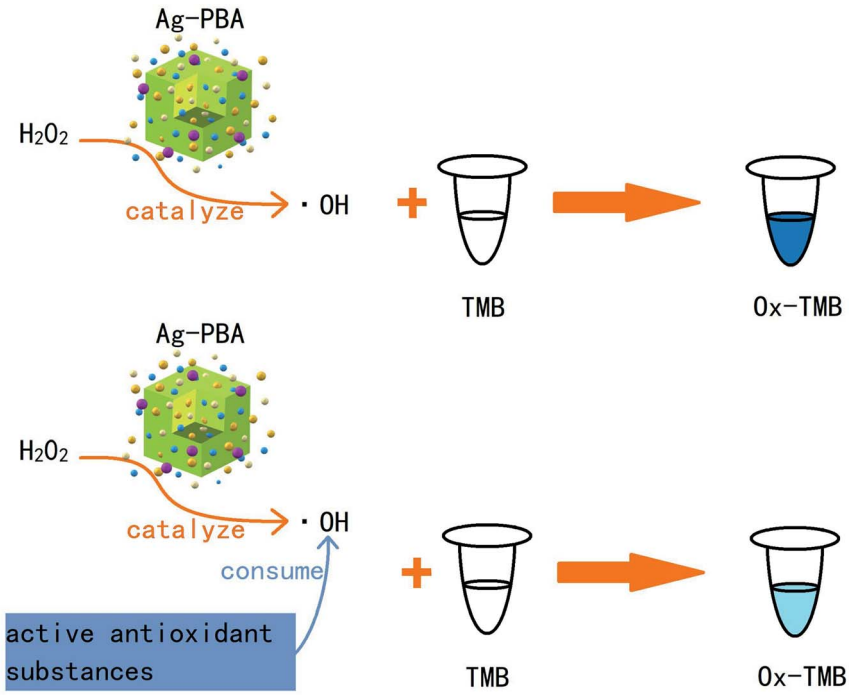

Scheme 1 Schematic illustration of the catalytic activity of Ag-PBA in the presence or absence of an active antioxidant substance.

flavonoids and have antioxidant, anti-free radical, and anti-aging activities. Currently, the rational use of active antioxidative substances can effectively prevent and treat some diseases and delay senescence.[38–41] The development of quantitative measurement methods for the content of antioxidant substances has become a key element in the research and development of antioxidant drugs.

At present, the content of antioxidant drugs can be measured by a variety of methods, including 1,1-diphenyl-2-picrylhydrazyl (DPPH) method, 2,2′-azino-bis(3-ethylbenzothiazoline-6-sulfonic acid) (ABTS) method, and the ferric reducing antioxidant potential (FRAP) method.[42] Although these methods have good functionality, they are not without their shortcomings. For example, the DPPH method must be performed in the absence of light, and the reaction time is more than 30 min. If batch determination is needed, a longer reaction time is required. Therefore, it is necessary to develop new methods that are rapid, simple, and economical.

As shown in Scheme 1, Ag-PBA can catalyze H_2O_2 to produce the hydroxyl radical (˙OH), which can oxidize TMB to produce a blue product, ox-TMB. However, when active antioxidant substances are added, they react with ˙OH, resulting in its consumption. Consequently, less TMB is oxidized to ox-TMB, and the solution is lighter blue in color. In this study, based on the peroxidase-like activity of Ag-PBA, a new method to measure the content of antioxidant substances in *L. ruthenicum* Murr. was developed. The method was compared with the DPPH method, and the reliability and feasibility of the method were statistically compared with the classical DPPH method. The new method offered the advantages of simplicity, rapidness, and good stability. It is expected to be adopted widely for the measurement of the content of antioxidant substances in TCMs.

2. Experimental section

2.1 Synthesis of Prussian blue analog (PBA) and Ag^+-decorated PBA (Ag-PBA)

First, 35 mg $Cu(CH_3COO)_2$, 150 mg PVP, and 220 mg $C_6H_5Na_3O_7 \cdot 2H_2O$ were dissolved in 10 mL deionized water to form solution 1. Then, 33 mg $CoCl_2 \cdot 2H_2O$, 150 mg PVP, and 219 mg $C_6H_5Na_3O_7 \cdot 2H_2O$ were dissolved in 10 mL deionized water to form solution 2, and 130 mg $K_3[Fe(CN)_6]$ was dissolved in 20 mL deionized water to form solution 3. After solutions 1 and 2 were mixed evenly, solution 3 was added dropwise into the mixture with stirring, which was continued for 0.5 h after the addition of solution 3. The stirred mixture was then kept at room temperature for 20 h and the color change was monitored. After the reaction was complete, the solution was centrifuged at 9500 rpm for 8 min. A water/ethanol mixture (1 : 1 volume ratio) and pure ethanol were used to wash the precipitate twice, respectively. The precipitate was dried, weighed, and then dissolved in 3 mL ethylene glycol. The concentration of PBA was 56.7 mg mL^{-1}.

To the obtained PBA solution, 10 mL $AgNO_3$ (2 mmol L^{-1}) solution was added dropwise, with stirring, over 3 h. Then, the solution was centrifuged at 9500 rpm for 8 min and washed with water and ethanol twice, respectively. The precipitate was dried, weighed, and then dissolved in 3 mL ethylene glycol. The concentration of Ag^+-decorated PBA (Ag-PBA) was 57.0 mg mL^{-1}.

2.2 Peroxidase-like activity of Ag-PBA and PBA

A mixture of 15 μL Ag-PBA (57.0 mg mL^{-1}) or PBA (56.7 mg mL^{-1}), 50 μL TMB (20 mmol L^{-1}), 50 μL H_2O_2 (50 mmol L^{-1}) and 1 mL phosphate buffer (pH 7.0) was prepared. The absorbance spectrum of the resulting solution was measured at 650 nm at 25 °C for 10 min. For the blank sample, 10 μL deionized water was added instead of PBA or Ag-PBA.

2.3 Application of Ag-PBA in the measurement of the concentration of the antioxidant substances in the ethanol extract of *L. ruthenicum* Murr.

2.3.1 Preparation of solutions of *L. ruthenicum* Murr. and the standard anthocyanidin solutions. *L. ruthenicum* Murr. was washed with deionized water and dried in a 50 °C oven until no further changes in weight occurred. When the *L. ruthenicum* Murr. was at room temperature, it was crushed with a grinder, and then passed through a 60-mesh sieve to collect the powder. Then, 200 g of the powder was weighed and 72% ethanol solution was added to achieve a liquid to material ratio of 18.9 mL g^{-1}.[43] The ethanol extract was obtained by ultrasonic extraction for 30 min (ultrasonic power: 300 W).[43] The solution was centrifuged at 9500 rpm for 5 min, and the supernatant was collected and the solvent was removed to yield the sample solution.

To prepare the anthocyanidin standard solution (50 mg mL^{-1}), 0.5000 g anthocyanidin powder was dissolved in 10.00 mL 95% ethanol.

2.3.2 Concentration of the antioxidant substances in the ethanol extract of *L. ruthenicum* Murr. measured by the Ag-PBA method. Ag-PBA can be used to activate the H_2O_2 oxidation of TMB, and the antioxidant substances in the ethanol extract of *L. ruthenicum* Murr., such as anthocyanidins, can consume $^{\cdot}OH$ produced by H_2O_2 in the reaction system, allowing their indirect quantification. This forms the basis of the Ag-PBA method for the quantitation of antioxidant substances.

2.3.2.1 Measurement of the concentration of the antioxidant substances in the sample solution by the Ag-PBA method

(1) The linear relationship between the concentration of the anthocyanidin standard solutions and absorbance. For the Ag-PBA method, 15 μL Ag-PBA (57 mg mL^{-1}), 38.5 μL TMB (20 mmol L^{-1}), 40 μL H_2O_2 (50 mmol L^{-1}), and 25 μL anthocyanidin standard solution at different concentrations and 981.5 μL phosphate buffer (pH 5.0) were mixed into the treatment solution, yielding final anthocyanidin concentrations of 0.025, 0.05, 0.1, 0.3, 0.5, 0.1, 1, 4, 7, 10, 13, 15 mg mL^{-1}. The absorbance of the solution was measured at 650 nm after the solution was incubated at 25 °C for 10 min. A linear relationship between the concentration of anthocyanidins solution and the absorbance was established and the linear regression equation was obtained.

(2) Concentration of the antioxidant substances in the sample solutions containing anthocyanidins. A mixture of 15 μL Ag-PBA (57.0 mg mL^{-1}), 38.5 μL TMB (20 mmol L^{-1}), 40 μL H_2O_2 (50 mmol L^{-1}), 25 μL sample solutions containing anthocyanidins, and 981.5 μL phosphate buffer (pH 5.0) was prepared. The absorbance of the solution was measured at 650 nm after incubation at 25 °C for 10 min. The concentration of antioxidant substances in the sample solution containing anthocyanidins was determined from the linear regression equation obtained in 2.3.2.1 (1).

2.3.3 Validating the results of the Ag-PBA method using the DPPH method. The concentration of the antioxidant substances in the ethanol extract of *L. ruthenicum* Murr. was measured by the DPPH method.[44] The DPPH solution was protected from light and freshly prepared just before use.

2.3.3.1 The linear relationship between the concentration of the anthocyanidin standard solutions and absorbance as measured by the DPPH method. For the DPPH method, 75 μL 95% ethanol, 25 μL standard solution with different concentrations of anthocyanidins and 1000 μL DPPH solution (0.1 mmol L^{-1}) were mixed into the treatment solution, yielding final anthocyanidins concentrations of 1, 4, 7, 10, 13, 15, 20 mg mL^{-1}. The absorbance of the solution was measured at 515 nm after incubation at 25 °C in the dark for 30 min. A linear relationship between the concentration of the anthocyanidins in solution and absorbance was established and the linear regression equation was obtained.

2.3.3.2 Concentration of the antioxidant substances in the sample solution compared with the standard anthocyanidin solutions as measured by the DPPH method. A mixture of 75 μL 95% ethanol, 25 μL ethanol extract solution of *L. ruthenicum* Murr., and 1000 μL DPPH solution (0.1 mmol L^{-1}) was mixed into the test solution. The absorbance of the solution was measured at 515 nm after incubation at 25 °C in the dark for 30 min. The

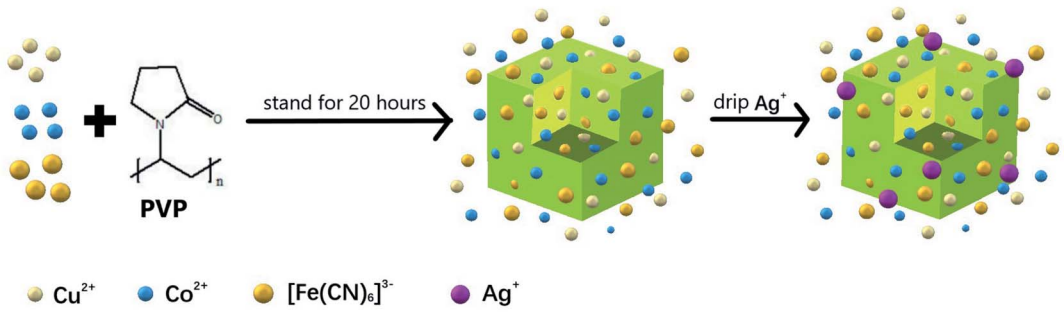

Scheme 2 The synthesis procedure for Ag-PBA.

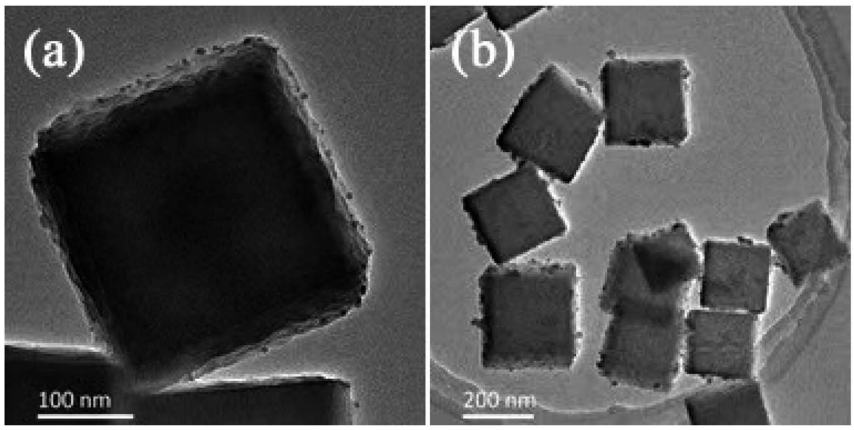

Fig. 1 TEM images of Ag-PBA. The scale bar represents (a) 100 nm and (b) 200 nm.

concentration of the antioxidant substances in the sample solution containing anthocyanidins was determined from the linear regression equation obtained above in 2.5.3.1.

2.3.3.3 Comparison of the concentration of the antioxidant substances in the sample solutions measured by the Ag-PBA and DPPH methods. To test the accuracy of the Ag-PBA method, the results of the Ag-PBA method and the DPPH method were compared by a paired *t*-test at the 0.05 level.

3. Results and discussion

3.1 Synthesis and characterization of Ag-PBA

PBA was synthesized in the presence of TSCD, which served as the controlling agent, and PVP, which served as the protective reagent. TSCD, as the reaction precursor, first reacts with the metal ions to form the metal-citrate complex, which slows down the reaction, leading to a preferentially oriented crystal growth.[28] The formed metal-citrate complex tended to release a few metal ions steadily and slowly when the $K_3[Fe(CN)_6]$ was added. Finally, the trimetallic PBA was synthesized by co-precipitation. The procedure is described in Scheme 2. PVP was used to prevent the accumulation of nanoparticles. Color changes in the solution during Ag-PBA synthesis are depicted in Fig. S1 (ESI†). As the reaction time increased, the color of the solution changed from green to yellow, and then gradually deepened. The resulting Ag-PBAs were purple (Fig. S1 and S2†). Transmission electron microscopy (TEM) images showed that Ag-PBAs were all of a cubic shape with a rough surface, and relatively uniform with a diameter of less than 250 nm (Fig. 1), indicating successful synthesis of Ag-PBA nanoenzymes. The Tyndall effect was used to confirm that the synthesized Ag-PBAs were of the order of nanometers in size (Fig. S3†). Scanning electron microscopy (SEM) images (Fig. 2) of Ag-PBAs and PBAs showed essentially the same cubic morphology, with a diameter of 200–250 nm, confirming the successful synthesis of Ag-PBA nanoparticles that retained a cubic crystalline structure and

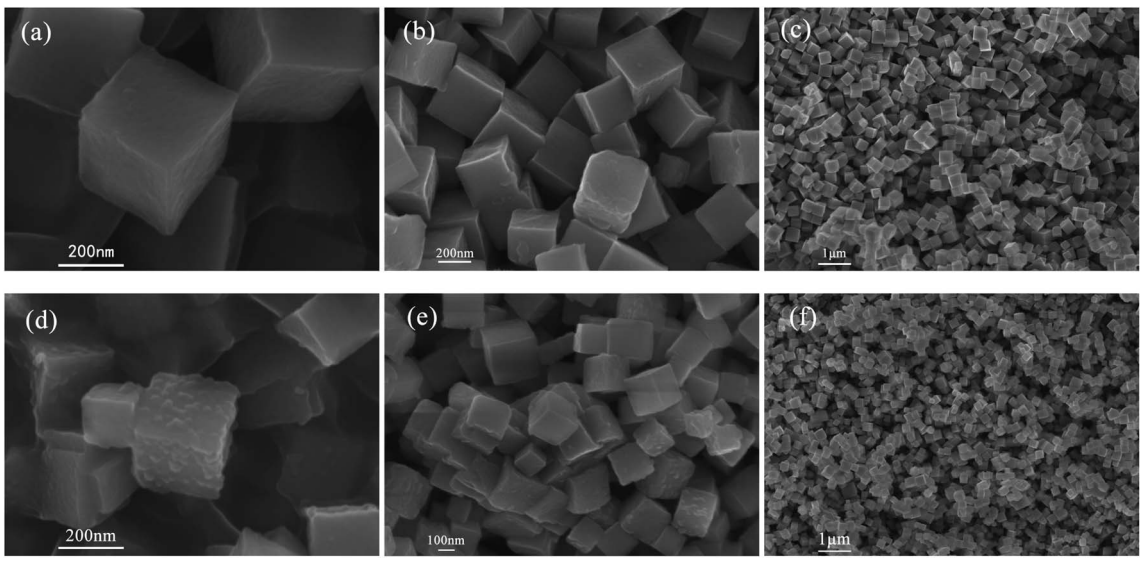

Fig. 2 SEM images of PBA. The magnification is (a) ×100 000, (b) ×50 000, and (c) ×10 000. SEM images of Ag-PBA. The magnification is (d) ×100 000, (e) ×50 000, and (f) ×10 000.

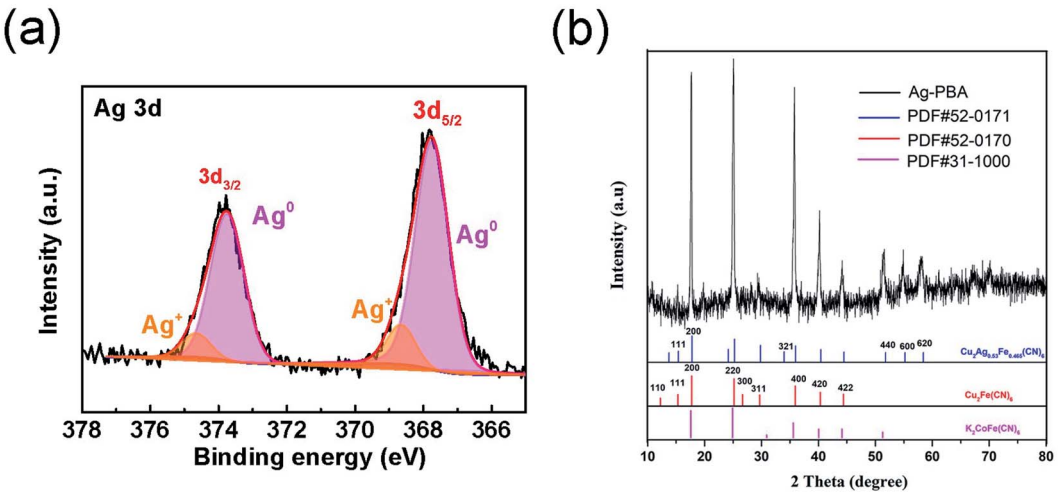

Fig. 3 (a) XPS Ag 3d spectrum of Ag-PBA; (b) XRD pattern of Ag-PBA.

a similar size to PBA. In the comparison of Fig. 2a with Fig. 2d, the surface of PBA was smooth, whereas the surface of Ag-PBA was relatively rough. To some extent, this phenomenon provided indirect proof that Ag^+ was successfully decorated on PBA, because it is very likely that Ag^+ binds to the surface of PBA, causing the surface to become rough. Further analysis was performed using elemental dispersive X-ray (EDX) spectroscopy. As shown in Fig. S4,† the EDX spectrum verified the presence of Ag in Ag-PBA, providing further confirmation that Ag^+ was successfully decorated on the PBA. The EDX results also showed the presence of C, N, O, Fe, Co, and Cu elements in both Ag-PBA and the PBA (Fig. S4 and S5†), indicating that a new trimetallic PBA was successfully synthesized. In addition, the mass fractions of C, N, O, Fe, Co, and Cu elements in the PBA and the mass fraction of Ag element in Ag-PBA are presented in Tables S1 and S2.† Furthermore, the chemical state of Ag was investigated with X-ray photoelectron spectroscopy (XPS). As shown in Fig. 3a, peak deconvolution revealed the contribution from both Ag and Ag^+.[45,46] The crystal structure of Ag-PBA was characterized by X-ray diffraction (XRD). The pattern for Ag-PBA (Fig. 3b) showed nine peaks at 12.253°, 15.318°, 17.740°, 25.187°, 26.669°, 29.680°, 35.928°, 40.328° and 44.380°, corresponding to (110), (111), (200), (220), (300), (311), (400), (420), and (422) of $Cu_2Fe(CN)_6$ (PDF #52-0170), respectively (Fig. 1b). This pattern contained a number of peaks that could be well-indexed to the crystalline phases of $Cu_2Ag_{0.53}Fe_{0.465}(CN)_6$ (PDF #52-0171) and $K_2CoFe(CN)_6$ (PDF #31-1000). Furthermore, as shown in Fig. S6,† the XRD patterns of Ag-PBA and PBA were well matched, indicating they had the same crystalline structure.

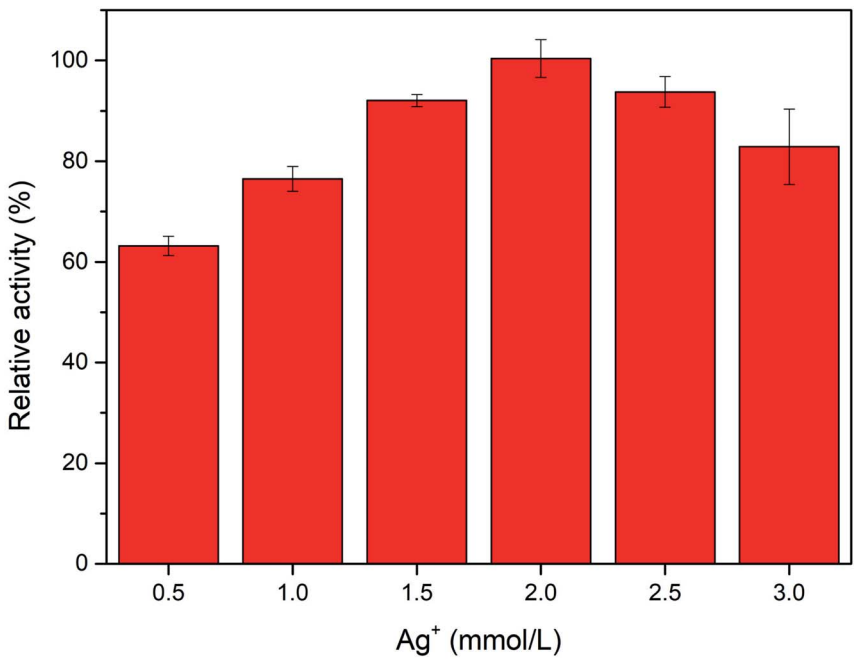

Fig. 4 Effect of the concentration of added Ag^+ on the catalytic activity of Ag-PBA ($n = 5$).

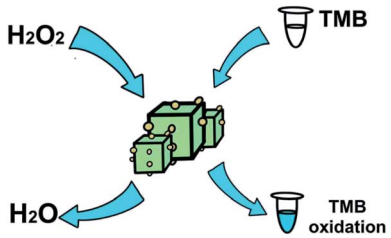

Scheme 3 Mechanism of the catalytic reaction based on Ag-PBA.

3.2 Optimization of the Ag^+ concentration for the synthesis of Ag-PBA

To obtain the Ag-PBA with the greatest catalytic activity, we investigated the effect of the concentration of Ag^+ added during the synthesis of Ag-PBA. As shown in Fig. 4, Ag-PBA has the best catalytic activity when the concentration of Ag^+ added during the synthesis process was 2.0 mmol L^{-1}. When the added Ag^+ concentration was too low, there were too few functional metal silver nanoparticles adsorbed on the cages or channels of the MOF structure of PBA; hence, the catalytic activity of the sample was not sufficiently improved. In contrast, when the added Ag^+ concentration was too high, silver nanoparticles were very likely not to be uniformly dispersed on PBAs during the process of silver dropping, which results in a lower adsorption capacity, fewer products, and decreased catalytic activity. Therefore, we selected a concentration of 2.0 mmol L^{-1} $AgNO_3$ for the synthesis of Ag-PBA.

3.3 Peroxidase-like activity of Ag-PBA

Prussian blue nanoparticles are characterized by the low energy orbitals available for the transfer of H_2O_2 electrons.[47] Ag-PBA, as a new type of PBA, also has this characteristic, and therefore has a superior affinity for H_2O_2. Thus, the Ag-PBA should also display peroxidase-like activity. To confirm the peroxidase-like activity of Ag-PBA, we used TMB as the substrate. The mechanism is shown in Scheme 3. As shown in Fig. 5, without PBA and Ag-PBA, the absorbance intensity of the solution was relatively low, and the curve was very flat. When the PBA was added, the absorbance intensity of the solution clearly increased over time owing to the generation of oxidized TMB. The addition of Ag-PBA increases the absorbance intensity of the solution to a greater extent, and the increase in absorbance was higher than that for PBA (Fig. 5). The results indicated that both PBA and Ag-PBA had peroxidase-like activity, and that the addition of Ag^+ increased the peroxidase-like activity of PBA. The mechanism through which Ag^+ enhanced the peroxidase-like activity was attributed to the naked catalytic surface with high catalytic activity provided by the Ag nanoparticles decorated on the PBA.[36] Thus, the anchoring of Ag^+ on the surface of PBAs was utilized to enhance the normalized activity of PBA.

3.4 Stability of Ag-PBA and PBA

First, we investigated the effects of pH on the peroxidase activity of Ag-PBA and PBA. As shown in Fig. 6a and e, when the pH of the solution was increased from 3 to 9, the catalytic activity of Ag-PBA and PBA first increased and then decreased, with a maximum activity at pH 5. This shows that the catalytic activity of Ag-PBA and PBA was strongly dependent on pH, and that Ag-PBA and PBA showed relatively good acid stability in the pH ranging of 4.0 to 7.0. Therefore, phosphate buffer (pH 5.0) was selected for subsequent experiments.

As the thermal stability of nano-enzymes is a crucial factor in an enzymic catalytic reaction, the thermal stability of Ag-PBA and PBA is of great importance. Thus, the thermal stability of Ag-PBA and PBA was investigated by incubating Ag-PBA and PBA samples at 10, 20, 30, 40, and 50 °C for 30 min, and then adding Ag-PBA or PBA into the reaction solution of 50 μL TMB (20 mmol L^{-1}) and 50 μL H_2O_2 (50 mmol L^{-1}) at 25 °C and

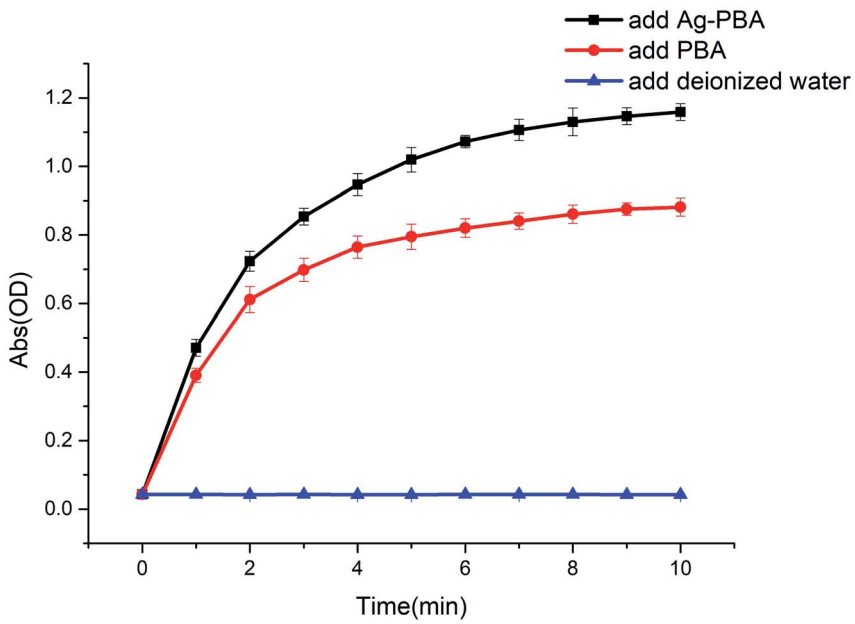

Fig. 5 Changes in the absorbance of solutions over time after the addition of deionized water, PBA, and Ag-PBA ($n = 5$).

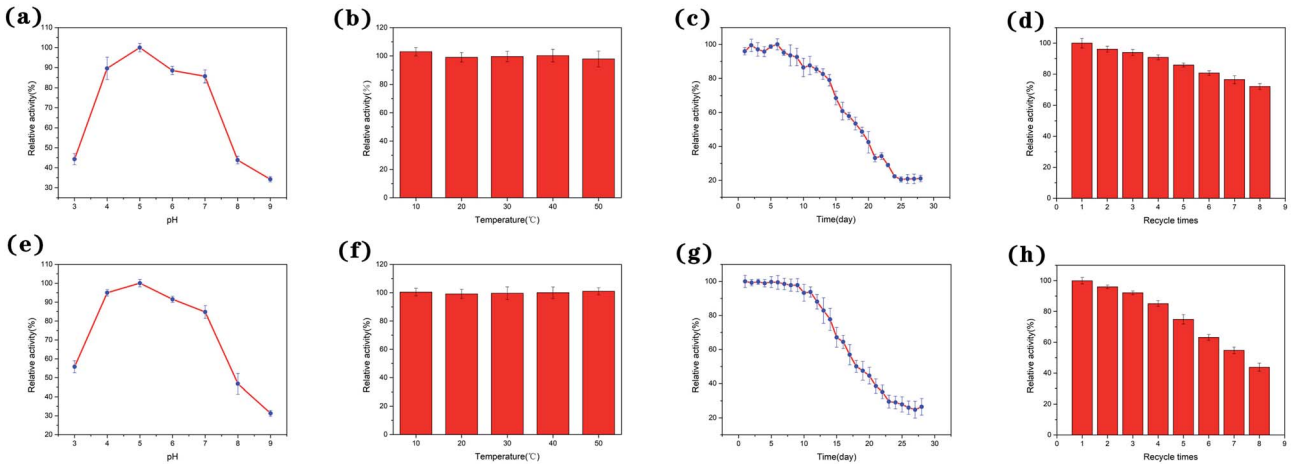

Fig. 6 Stability of Ag-PBA and PBA ($n = 5$), the stability to (a) pH, (b) temperature, and (c) storage, (d) and reusability of Ag-PBA. The stability to (e) pH, (f) temperature, and (g) storage, and (h) reusability of PBA.

measuring the enzyme activity. The results are shown in Fig. 6b and f: Ag-PBA and PBA exhibited good thermal stability over the temperature range tested.

The stability of Ag-PBA and PBA to storage was evaluated. As shown in Fig. 6c, Ag-PBA retained its original catalytic activity for 9 days and maintained 50% of its initial activity after 18 days. However, after 24 days, Ag-PBA lost almost all activity. It can be concluded that the quality of Ag-PBA is guaranteed for approximately 9 days, and the catalytic activity decreases slowly after this time. As shown in Fig. 6g, PBA retained its original catalytic activity for 8 days and maintained 50% of its initial activity after 18 days. After 23 days, PBA lost almost all activity. It can be concluded that the quality of PBA is guaranteed for approximately 8 days, and the catalytic activity decreases slowly after this time.

For economic reasons, the ability to reuse nano-enzymes is also a vital consideration in their practical application. The reusability of Ag-PBA and PBA was measured. As shown in Fig. 6d and h, Ag-PBA retained approximately 72% of its initial catalytic activity after eight cycles; however, the relative activity of PBA decreased to approximately 43%. The increased reusability after anchoring of Ag^+ on the surface of PBA may be due to the protection afforded by Ag^+, which decreases the loss of PBA during the recovery process.

Ag-PBA and PBA both have peroxidase-like activity. In addition, both compounds have strong catalytic activity at pH 5.0, good thermal stability, and retain 50% of their catalytic activity when stored at room temperature for 18 days. However, Ag-PBA has higher reusability; after 8 cycles, Ag-PBA retains 80% of its catalytic activity, whereas PBA retains only 50% of its catalytic activity.

3.5 Concentration of the antioxidant substances in the ethanol extract solution of *L. ruthenicum* Murr. calculated by the Ag-PBA method

As shown in Fig. S7,† the electron paramagnetic resonance (EPR) spectrum verified the existence of a specific ROS (the hydroxyl radical, ·OH) in the Ag-PBA–H_2O_2–TMB system,[48,49] indicating that Ag-PBA could catalyze H_2O_2 to produce ·OH. This also indirectly confirmed the rationale for the Ag-PBA method, because the anthocyanidins could interact quantitatively with ·OH and could be indirectly quantified through the color change in TMB.

3.5.1 Optimization of the conditions for Ag-PBA catalysis.

To determine the optimal reaction conditions, we investigated the influence of the reaction temperature, TMB and H_2O_2 concentration and reaction time on the catalysis. First, we investigated the effects of reaction temperature on the peroxidase-like activity of Ag-PBA. As shown in Fig. 7a, Ag-PBA exhibited stable and high catalytic activity over a wide temperature range (20–50 °C). Therefore, we chose 25 °C as the test temperature at which the antioxidant activity was measured using the Ag-PBA method in subsequent experiments.

Next, we investigated the effects of TMB concentration on the peroxidase-like activity of Ag-PBA. As shown in Fig. 7b, at 2.27 mmol L^{-1} H_2O_2, the absorbance of the solution increased rapidly as the concentration of TMB was increased from 0.1 to 0.7 mmol L^{-1}, and then reached a plateau. This indicated that 2.27 mmol L^{-1} H_2O_2 could oxidize 0.7 mmol L^{-1} TMB to ox-TMB (blue) when catalyzed by Ag-PBA. Hence, 0.7 mmol L^{-1} TMB was chosen for the catalytic reaction of Ag-PBA in the subsequent experiments.

The effect of H_2O_2 concentration on the peroxidase-like activity of Ag-PBA was then investigated. As shown in Fig. 7c, at 0.7 mmol L^{-1} TMB, the absorbance of the solution increased rapidly as the H_2O_2 concentration was increased from 0.45 to 1.82 mmol L^{-1}, and then reached a plateau. This indicated that Ag-PBA could completely catalyze approximately 1.82 mmol L^{-1} H_2O_2 to produce ·OH, which was sufficient to oxidize 0.7 mmol L^{-1} TMB to ox-TMB (blue) in just 10 min. Therefore, 1.82 mmol L^{-1} H_2O_2 was chosen for the catalytic reaction of Ag-PBA in the subsequent experiments.

The reaction time directly affects the results of the experiment. Thus, it is necessary to investigate the influence of reaction time on the Ag-PBA catalysis. The results are shown in Fig. 7d; the test was conducted as described in the ESI.† The inhibition efficiency increased rapidly in the first 5 min, then slowed, and reached a plateau after 10 min; the subsequent changes that occurred were slow. Therefore, to ensure a complete reaction over a short time, 10 min was selected for the subsequent experiments.

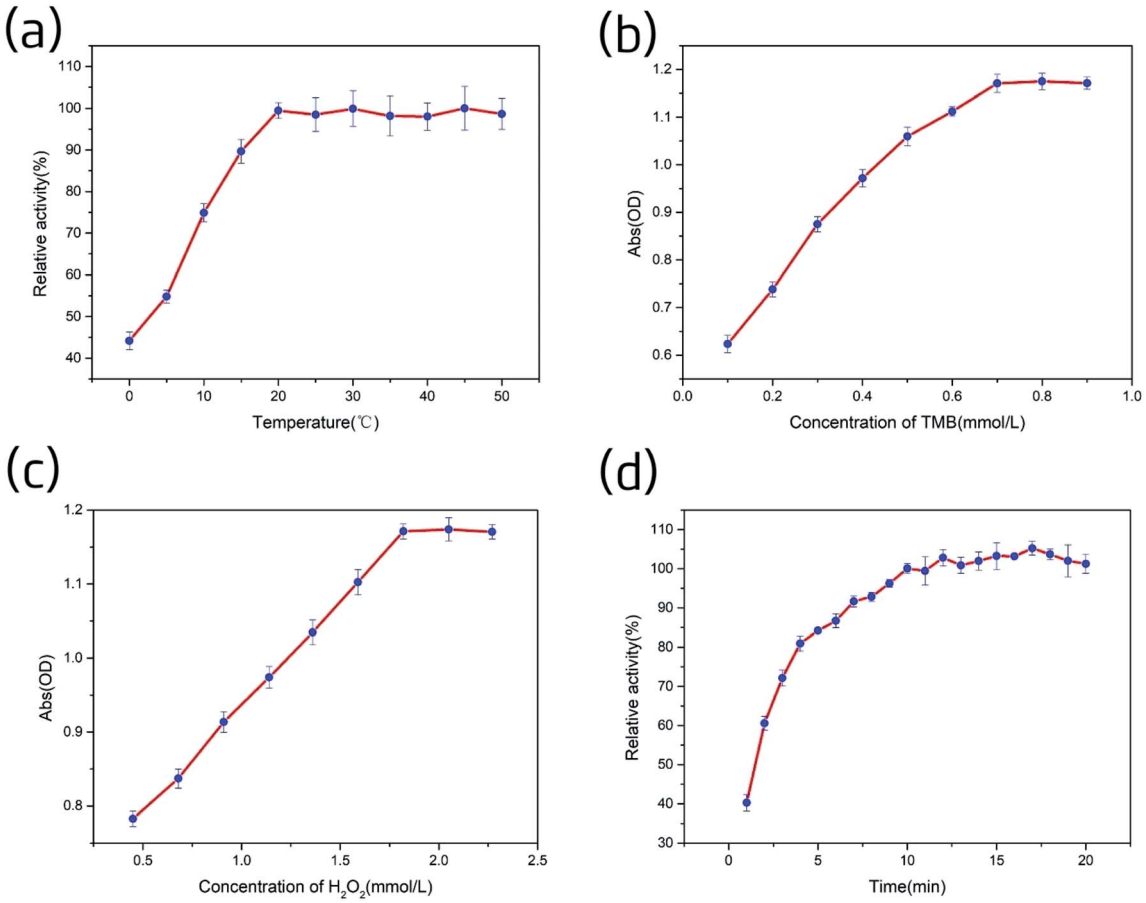

Fig. 7 Effects of reaction temperature, TMB and H_2O_2 concentrations, and the reaction time on the catalytic activity of Ag-PBA ($n = 5$). Variation of (a) reaction temperature, (b) TMB, (c) H_2O_2, and (d) reaction time.

3.5.2 Potential sources of interference in the Ag-PBA method

3.5.2.1 Interference by reducing substances. The mechanism of the Ag-PBA method is the quantitative interaction of anthocyanidins with $^{\bullet}OH$ produced by H_2O_2 in the Ag-PBA–H_2O_2–TMB reaction system, which allows indirect quantification through detection of the color change in the solution. Therefore, other reducing substances may interfere with the Ag-PBA method through their reaction with $^{\bullet}OH$, including Fe^{2+}, ascorbic acid, and glutathione. Therefore, we investigated potential sources of interference in the Ag-PBA method. As shown in Fig. 8, we studied the effects of Fe^{2+} and ascorbic acid. Compared with the blank group, the absorbance values of the experimental groups were notably decreased observably owing to the interaction of Fe^{2+} and ascorbic acid with $^{\bullet}OH$. These observations indicated that reducing substances, such as Fe^{2+} and ascorbic acid, would interfere with the Ag-PBA method. Therefore, when using the Ag-PBA method for quantitative detection, special attention should be paid to potential interference from reducing substances that can react with $^{\bullet}OH$.

3.5.2.2 Interference resulting from Ag^+ dissolution in the phosphate buffer solution. At an $AgNO_3$ concentration of 1.1×10^{-3} mmol L^{-1}, a brick-red precipitate appeared in the 5 mL phosphate buffer (pH 5.0) containing 1 mol L^{-1} K_2CrO_4.

First, 60 mg Ag-PBA powder was added into 5 mL phosphate buffer solution (pH 5.0) containing 1 mol L^{-1} K_2CrO_4 and the solution was left to stand for 1 h. No brick-red precipitation was formed, suggesting that the concentration of dissolved Ag^+ was less than 1.1×10^{-3} mmol L^{-1} when Ag-PBA was added into phosphate buffer solution (pH 5.0). For the Ag-PBA method, a low concentration of Ag was used, and the negligible interference with the experimental results occurred. These results also confirmed that Ag-PBA had very high stability in the experimental system, with Ag^+ anchored firmly on the surface of PBA.

3.5.3 The linear relationship between the concentration of the anthocyanidin standard solutions and absorbance measured by the Ag-PBA method. The linear relationship between anthocyanidin concentration and absorbance was investigated as described in the Experimental section; the results are shown in Fig. 9a and b. The absorbance decreased linearly as the anthocyanidin concentration increased from 0.1 to 15 mg mL^{-1}. The linear regression equation was $Y = -0.0723X + 1.15774$; $r^2 = 0.99938$.

As shown in Fig. 8b, when the anthocyanidins concentration was below 0.1 mg mL^{-1}, the average absorbance was larger and a sharp upward curve, no longer linear, was observed. Hence, the limit of quantification of the Ag-PBA method was determined to be 0.1 mg mL^{-1}.

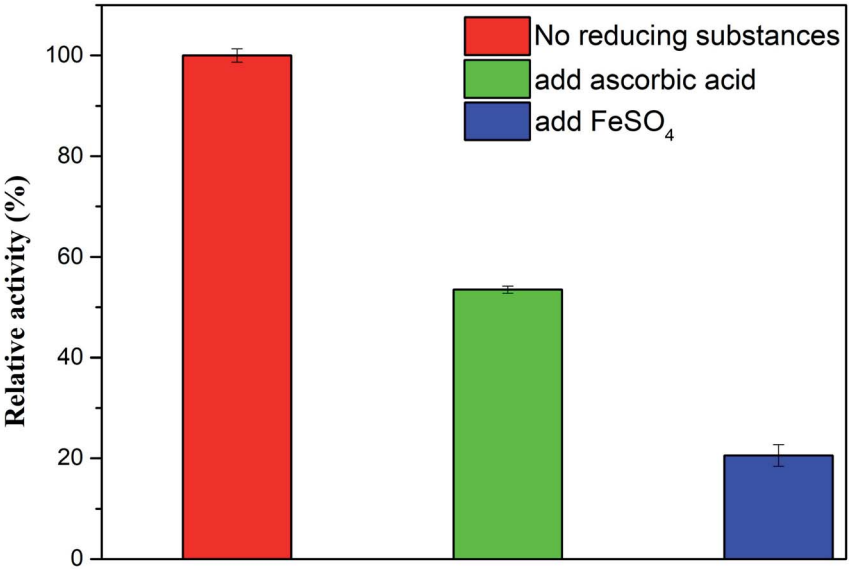

Fig. 8 The interference of reducing substances in the Ag-PBA method.

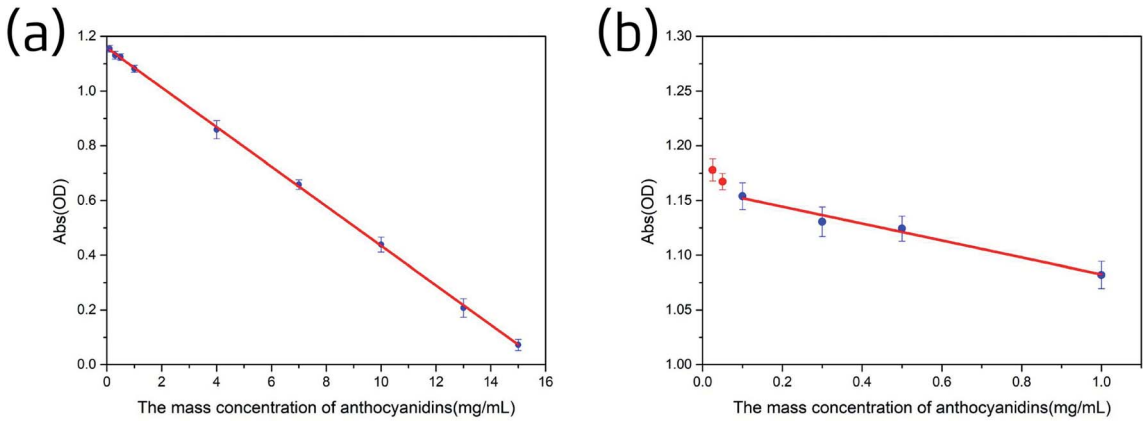

Fig. 9 Changes in absorbance related to anthocyanidin concentration as measured by the Ag-PBA method (n = 5). The anthocyanidin concentrations presented are (a) 0.1–15 mg mL^{-1} and (b) 0.025–1.0 mg mL^{-1}.

3.5.4 Concentration of antioxidant substances in the ethanol extract solution calculated in comparison with standard anthocyanidin solutions measured by the Ag-PBA method. The absorbance of five sample solutions was measured five times as described in the Experimental section; the results are shown in Table S3.† We calculated the concentration of the antioxidant substances in the sample solutions with anthocyanidins by using the linear regression equation presented above, $Y = -0.0723X + 1.15774$. The concentration of the antioxidant in the five sample solutions containing anthocyanidins was 13.72, 11.17, 7.40, 5.02, and 1.86 mg mL^{-1}, respectively.

3.5.5 Validation of the Ag-PBA method using the DPPH method

3.5.5.1 Qualitative comparison of the antioxidant activity of anthocyanidins measured by the Ag-PBA method and the DPPH method. The Ag-PBA method and the DPPH method were used to determine the antioxidant activity of anthocyanidins; the results are shown in Fig. S8.† For both methods, after the anthocyanidins were added, the color of the solution became lighter, indicating that the anthocyanidins had antioxidant activity. It was therefore possible to quantify the anthocyanidin concentration in the subsequent experiments by measuring the color change in the solution.

3.5.5.2 The linear relationship between the concentration of anthocyanidins in solution and absorbance measured by the DPPH method. A linear relationship between the concentration of the anthocyanidins in solution and the absorbance was established as described in the Experimental section. The results are shown in Fig. 10. We observed a linear decrease in absorbance as the anthocyanidin concentration increased from 1.0 to 20 mg mL^{-1}. The linear regression equation was $Y = -0.08126X + 1.80704$; $r^2 = 0.99926$.

3.5.5.3 Concentration of antioxidant substances in the sample solutions calculated in comparison with standard anthocyanidin

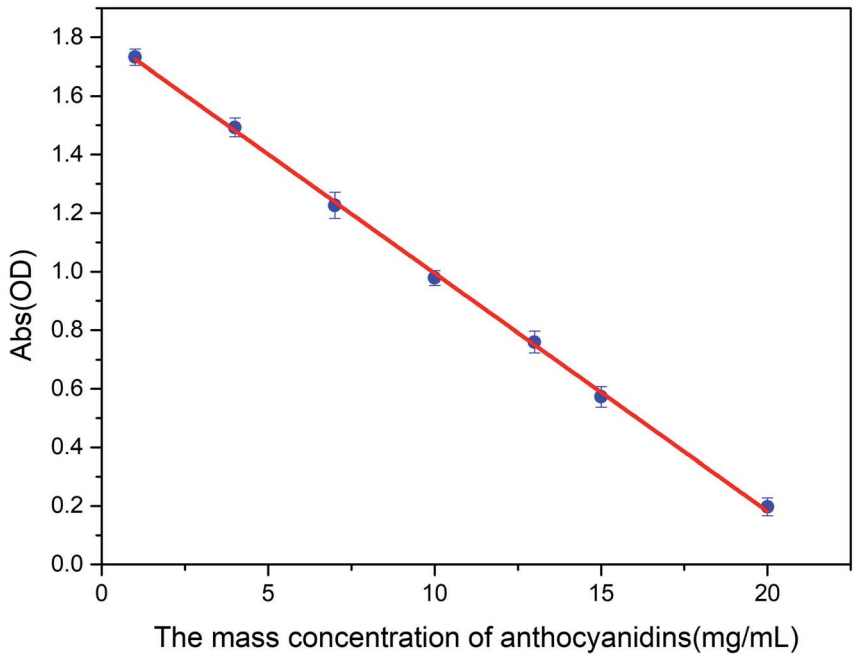

Fig. 10 Changes in absorbance as the anthocyanidin concentration increased, as measured by the DPPH method ($n = 5$).

Table 1 Comparison between the Ag-PBA method and the DPPH method

Method	Linear range	Reaction time	Limitation	Reaction mechanism
DPPH	1.0–20 mg mL^{-1}	30 min	Need to avoid light	Quantitative action with DPPH radical
Ag-PBA	0.1–15 mg mL^{-1}	10 min	None	Quantitative interaction with $^{\cdot}OH$

solutions measured by the DPPH method. The absorbance of five sample solutions of the ethanol extracts of *Lycium ruthenicum* Murr. was measured five times as described in the Experimental section; the results are shown in Table S3.† The concentration of the antioxidant substances in the sample solutions with anthocyanidins was calculated by using the linear regression equation presented above, $Y = -0.08126X + 1.80704$. The concentration of antioxidant substances of the five sample solutions calculated with anthocyanidins was 13.96, 10.97, 7.21, 4.91, and 1.69 mg mL^{-1}.

3.5.5.4 Significance test of the results measured by the above two methods. A paired *t*-test was used to examine the significance of any differences in the results of the two methods. The calculated concentrations from the two methods were imported into SPSS software and analyzed by a paired *t*-test. At the $\alpha = 0.05$ level, there was no significant difference between the two methods ($P = 0.359$).

3.5.5.5 Potential advantages of the Ag-PBA method over the DPPH method for practical applications. A comparison of the Ag-PBA method and the DPPH method is presented in Table 1. The Ag-PBA method has many obvious advantages that will support its practical application: notably, there is no need to avoid light, and the reaction time is shorter.

4. Conclusions

We successfully synthesized a new PBA with peroxidase-like activity by using a simple, convenient, economical, and environmentally friendly method. We found that the anchoring of Ag^{+} on the surface of the PBA enhanced the peroxidase-like activity of the material. Ag-PBA exhibited excellent thermostability, storability, reusability, and excellent acid resistance between pH 4.0 and 7.0. Thus, this represents an efficient strategy for the preparation of Ag-PBA with high peroxidase-like activity. Ag-PBA has potential applications in many fields, including traditional Chinese medicine. We developed a new method to measure the content of the antioxidant substances in Chinese herbs based on the peroxidase-like activity of Ag-PBA. After optimization of the reaction temperature, TMB and H_2O_2 concentrations, and reaction time, the content of the antioxidant substances in *L. ruthenicum* Murr. was measured by the Ag-PBA method. There were no significant differences in the results obtained with those of the classical DPPH method. Therefore, the two methods are interchangeable, but the Ag-PBA method has the advantages of simplicity, rapidness, and good stability. We anticipate that the Ag-PBA method can be used to detect the content of antioxidant substances in other Chinese herbs.

Conflicts of interest

There are no conflicts to declare.

Acknowledgements

This work was financially supported by The National Key Research and Development Program of China, No. 2019YFC1711200.

Notes and references

1 R. Wolfenden and M. J. Snider, *Acc. Chem. Res.*, 2001, **34**, 938–945.
2 L. Z. Hu, H. Liao, L. Y. Feng, M. Wang and W. S. Fu, *Anal. Chem.*, 2018, **90**, 6247–6252.
3 J. J. X. Wu, X. Y. Wang, Q. Wang, Z. P. Lou, S. R. Li, Y. Y. Zhu, L. Qin and H. Wei, *Chem. Soc. Rev.*, 2019, **48**, 1004–1076.
4 X. Y. Wang, Y. H. Hu and H. Wei, *Inorg. Chem. Front.*, 2016, **3**, 41–60.
5 Q. M. Chen, S. Q. Li, Y. Liu, X. D. Zhang, Y. Tang, H. X. Chai and Y. M. Huang, *Sens. Actuators, B*, 2020, **305**, 9.
6 B. W. Liu and J. W. Liu, *Nano Res.*, 2017, **10**, 1125–1148.
7 A. A. Karyakin, *Electroanalysis*, 2001, **13**, 813–819.
8 J. F. Keggin and F. D. Miles, *Nature*, 1936, **137**, 577–578.
9 F. Herren, P. Fischer, A. Ludi and W. Haelg, *Inorg. Chem.*, 1980, **19**, 956–959.
10 L. Wang, Y. Han, X. Feng, J. Zhou and P. Qi, *Coord. Chem. Rev.*, 2016, **307**, 361–381.
11 C. L. Zhang, Y. Xu, M. Zhou, L. Y. Liang, H. S. Dong, M. H. Wu, Y. Yang and Y. Lei, *Adv. Funct. Mater.*, 2017, **27**, 8.
12 P. L. dos Santos, V. Katic and K. C. F. Toledo, *Sens. Actuators, B*, 2018, **255**, 2437–2447.
13 P. C. Pandey and A. K. Pandey, *Electrochim. Acta*, 2014, **125**, 465–472.
14 X. J. Cai, W. Gao, M. Ma, M. Y. Wu, L. L. Zhang, Y. Y. Zheng, H. R. Chen and J. L. Shi, *Adv. Mater.*, 2015, **27**, 6382–6389.
15 Z. G. Qin, Y. Li and N. Gu, *Adv. Healthcare Mater.*, 2018, **7**, 13.
16 W. Zhang, S. L. Hu, J. J. Yin, W. W. He, W. Lu, M. Ma, N. Gu and Y. Zhang, *J. Am. Chem. Soc.*, 2016, **138**, 5860–5865.
17 P. J. Ni, Y. J. Sun, H. C. Dai, W. D. Lu, S. Jiang, Y. L. Wang, Z. Li and Z. Li, *Sens. Actuators, B*, 2017, **240**, 1314–1320.
18 S. Q. Li, X. D. Liu, H. X. Chai and Y. M. Huang, *TrAC, Trends Anal. Chem.*, 2018, **105**, 391–403.
19 W. M. Zhang, D. Ma and J. X. Du, *Talanta*, 2014, **120**, 362–367.
20 M. Vazquez-Gonzalez, R. M. Torrente-Rodriguez, A. Kozell, W. C. Liao, A. Cecconello, S. Campuzano, J. M. Pingarron and I. Willner, *Nano Lett.*, 2017, **17**, 4958–4963.
21 W. Xia, A. Mahmood, R. Q. Zou and Q. Xu, *Energy Environ. Sci.*, 2015, **8**, 1837–1866.
22 Q. M. Chen, X. D. Zhang, S. Q. Li, J. K. Tan, C. J. Xu and Y. M. Huang, *Chem. Eng. J.*, 2020, **395**, 10.
23 H. J. Cheng, Y. F. Liu, Y. H. Hu, Y. B. Ding, S. C. Lin, W. Cao, Q. Wang, J. J. X. Wu, F. Muhammad, X. Z. Zhao, D. Zhao, Z. Li, H. Xing and H. Wei, *Anal. Chem.*, 2017, **89**, 11552–11559.
24 M. B. Zakaria and T. Chikyow, *Coord. Chem. Rev.*, 2017, **352**, 328–345.
25 L. Catala and T. Mallah, *Coord. Chem. Rev.*, 2017, **346**, 32–61.
26 F. X. Bu, C. J. Du, Q. H. Zhang and J. S. Jiang, *CrystEngComm*, 2014, **16**, 3113–3120.
27 H. Ming, N. L. K. Torad, Y. D. Chiang, K. C. W. Wu and Y. Yamauchi, *CrystEngComm*, 2012, **14**, 3387–3396.
28 M. B. Zakaria, C. Li, P. Malay, Y. Tsujimoto and Y. Yamauchi, *J. Mater. Chem. A*, 2016, **4**, 9266–9274.
29 M. B. Zakaria, V. Malgras, T. Takei, C. L. Li and Y. Yamauchi, *Chem. Commun.*, 2015, **51**, 16409–16412.
30 C. Qi, S. F. Cai, X. H. Wang, J. Y. Li, Z. Lian, S. S. Sun, R. Yang and C. Wang, *RSC Adv.*, 2016, **6**, 54949–54955.
31 C. Rosler and R. A. Fischer, *CrystEngComm*, 2015, **17**, 199–217.
32 N. Bagheri, A. Khataee, B. Habibi and J. Hassanzadeh, *Talanta*, 2018, **179**, 710–718.
33 N. Bagheri, A. Khataee, J. Hassanzadeh and B. Habibi, *J. Hazard. Mater.*, 2018, **360**, 233–242.
34 J. Jin, S. J. Zhu, Y. B. Song, H. Y. Zhao, Z. Zhang, Y. Guo, J. B. Li, W. Song, B. Yang and B. Zhao, *ACS Appl. Mater. Interfaces*, 2016, **8**, 27956–27965.
35 S. Kumar, P. Bhushan and S. Bhattacharya, *RSC Adv.*, 2017, **7**, 37568–37577.
36 J. Ju, R. Z. Zhang and W. Chen, *Sens. Actuators, B*, 2016, **228**, 66–73.
37 J. Zheng, C. X. Ding, L. S. Wang, G. L. Li, J. Y. Shi, H. Li, H. L. Wang and Y. R. Suo, *Food Chem.*, 2011, **126**, 859–865.
38 H. Ichikawa, T. Ichiyanagi, B. Xu, Y. Yoshii, M. Nakajima and T. Konishi, *J. Med. Food*, 2001, **4**, 211.
39 S. Lamy, M. Blanchette, J. Michaud-Levesque, R. Lafleur, Y. Durocher, A. Moghrabi, S. Barrette, D. Gingras and R. Beliveau, *Carcinogenesis*, 2006, **27**, 989–996.
40 M. M. Rahman, T. Ichiyanagi, T. Komiyama, S. Sato and T. Konishi, *J. Agric. Food Chem.*, 2008, **56**, 7545.
41 H. Wang, G. Cao and R. L. Prior, *J. Agric. Food Chem.*, 1997, **45**, 304–309.
42 N. Pellegrini, P. Vitaglione, D. Granato and V. Fogliano, *J. Sci. Food Agric.*, 2020, **100**, 5064–5078.
43 L. Y. Zhang and H. Q. Wang, *Food Ind.*, 2014, **35**, 88–91.
44 M. S. Blois, *Nature*, 1958, **181**, 1199–1200.
45 W. J. Huang, X. L. Kang, C. Xu, J. H. Zhou, J. Deng, Y. G. Li and S. Cheng, *Adv. Mater.*, 2018, **30**, 6.
46 V. K. Kaushik, *J. Electron Spectrosc. Relat. Phenom.*, 1991, **56**, 273–277.
47 Y. Zhou, *Prepartion of Prussian blue nanomaterials and their application in glucose detection*, Southeast University, 2014.
48 R. Amarowicz, R. B. Pegg, P. Rahimi-Moghaddam, B. Barl and J. A. Weil, *Food Chem.*, 2004, **84**, 551–562.
49 V. E. Kagan, Y. Y. Tyurina, V. A. Tyurin, N. V. Konduru, A. I. Potapovich, A. N. Osipov, E. R. Kisin, D. Schwegler-Berry, R. Mercer, V. Castranova and A. A. Shvedova, *Toxicol. Lett.*, 2006, **165**, 88–100.